Doxazosin inhibits vasculogenic mimicry in human non-small cell lung cancer through inhibition of the VEGF-A/VE-cadherin/mTOR/MMP pathway

JUI-LING HSU[1-3], WOHN-JENN LEU[2], LIH-CHING HSU[2], CHIA-HSUN HSIEH[3-5] and JIH-HWA GUH[2]

[1]Department of Nursing, Division of Basic Medical Sciences, Chang-Gung University of Science and Technology, Taoyuan 333; [2]School of Pharmacy, College of Medicine, National Taiwan University, Taipei 100; [3]Division of Hematology-Oncology, Department of Internal Medicine, New Taipei Municipal TuCheng Hospital, New Taipei City 236; [4]Division of Medical Oncology, Department of Internal Medicine, Chang Gung Memorial Hospital at Linkou; [5]College of Medicine, Chang Gung University, Taoyuan 333, Taiwan, R.O.C.

Received September 22, 2023; Accepted January 25, 2024

DOI: 10.3892/ol.2024.14303

Abstract. Lung cancer is the leading cause of cancer-related death worldwide, and ~85% of lung cancers are non-small cell lung cancer (NSCLC), which has a low 5-year overall survival rate and high mortality. Several therapeutic strategies have been developed, such as targeted therapy, immuno-oncotherapy and combination therapy. However, the low survival rate indicates the urgent need for new NSCLC treatments. Vasculogenic mimicry (VM) is an endothelial cell-free tumor blood supply system of aggressive and metastatic tumor cells present during tumor neovascularization. VM is clinically responsible for tumor metastasis and resistance, and is correlated with poor prognosis in NSCLC, making it a potential therapeutic target. In the present study, A549 cells formed glycoprotein-rich lined tubular structures, and transcript levels of VM-related genes were markedly upregulated in VM-forming cells. Based on a drug repurposing strategy, it was demonstrated that doxazosin (an antihypertensive drug) displayed inhibitory activity on VM formation at non-cytotoxic concentrations. Doxazosin significantly reduced the levels of vascular endothelial growth factor A (VEGF-A) and matrix metalloproteinase-2 (MMP-2) in the cell media during VM formation. Further experiments revealed that the protein expression levels of VEGF-A and vascular endothelial-cadherin (VE-cadherin), which contribute to tumor aggressiveness and VM formation, were downregulated following doxazosin treatment. Moreover, the downstream signaling Ephrin type-A receptor 2 (EphA2)/AKT/mTOR/MMP/Laminin-5γ2 network was inhibited in response to doxazosin treatment. In conclusion, the present study demonstrated that doxazosin displayed anti-VM activity in an NSCLC cell model through the downregulation of VEGF-A and VE-cadherin levels, and the suppression of signaling pathways related to the receptor tyrosine kinase, EphA2, protein kinases, AKT and mTOR, and proteases, MMP-2 and MMP-9. These results support the add-on anti-VM effect of doxazosin as a potential agent against NSCLC.

Correspondence to: Dr Jui-Ling Hsu, Department of Nursing, Division of Basic Medical Sciences, Chang-Gung University of Science and Technology, 261 Wenhua 1st Road, Guishan, Taoyuan 333, Taiwan, R.O.C.
E-mail: jlhsu@mail.cgust.edu.tw

Dr Jih-Hwa Guh, School of Pharmacy, College of Medicine, National Taiwan University, 33 Linsen S. Road, Zhongzheng, Taipei 100, Taiwan, R.O.C.
E-mail: jhguh@ntu.edu.tw

Key words: non-small cell lung cancer, vasculogenic mimicry, doxazosin, drug repurposing, vascular endothelial growth factor A/vascular endothelial-cadherin pathway

Introduction

Lung cancer is the leading cause of cancer-related death worldwide. Non-small cell lung cancer (NSCLC), including adenocarcinoma, squamous cell carcinoma and large cell carcinoma, comprises ~85% of all lung cancer cases (1,2). Advances in recent decades have led to the identification of numerous oncogenic factors in NSCLC, such as gene mutations in *EGFR*, *BRAF*, ROS proto-oncogene 1, $p16^{INK4a}$ and human epidermal growth factor receptor 2, and rearrangements in anaplastic lymphoma kinase and *RET* (3-6) Although target therapies and immunotherapies have enhanced the overall survival time of patients, the occurrence of metastasis and resistance (primary or acquired) may cause difficulties for effective second-line treatment options. This has resulted in an urgent unmet need for NSCLC treatment (7).

Vasculogenic mimicry (VM), a new blood supply network with abundant extracellular matrix (ECM), is the formation of microvascular channels by aggressive and metastatic tumor cells (8). VM is suggested to be responsible for tumor metastasis and poor prognosis in patients with cancer, such as lung cancer, colorectal cancer, liver cancer, sarcoma and

melanoma (8-10). VM offers functional perfusion pathways for rapidly growing tumors by transferring fluid from leaky vessels and connecting with vasculature, representing a non-angiogenic pathway. Aggressive tumors possess VM structures, which are inaccessible to anti-angiogenic therapies, resulting in cancer resistance (11,12). Analysis of NSCLC tissue samples has indicated that the levels of VM, slug and vimentin [two key regulators in epithelial-mesenchymal transition (EMT)] are higher in NSCLC tissues compared with normal lung tissues (13,14). Furthermore, CDK5 kinase induces focal adhesion kinase (FAK)/AKT signaling and subsequent VM formation. Blockade of CDK5 by inhibitors or siRNA inhibits VM formation and tumor growth in an NSCLC A549 cell line and animal models (15).

Drug repurposing has emerged as an attractive approach in combating malignant tumors (16-19). Doxazosin, an α1-adrenergic blocker for the treatment of hypertension and the symptoms of benign prostatic hyperplasia, has been reported to display anticancer activity through the inhibition of cell proliferation, migration and metastasis, and the induction of autophagy and apoptosis of cancer cells (20-23). Furthermore, doxazosin is reported to inhibit vascular endothelial growth factor (VEGF), suppressing the migration and invasion of endothelial cells (24). However, the impact of doxazosin on VM formation has not yet, to the best of our knowledge, been reported. In the present study, a VM model containing hollow lumens was established using an NSCLC cell model and the inhibitory activity of doxazosin was studied. To the best of our knowledge, the present study is the first report to elucidate the anti-VM effect of doxazosin.

Materials and methods

Materials. The human NSCLC cell line, A549, was purchased from the American Type Culture Collection. RPMI 1640 medium, fetal bovine serum (FBS), penicillin and streptomycin were purchased from Gibco (Thermo Fisher Scientific, Inc.). The GAPDH (cat. no. 32233) and fibronectin (cat. no. 18825) antibodies were purchased from Santa Cruz Biotechnology, Inc. Vascular endothelial (VE)-cadherin (cat. no. 2500), Ephrin type-A receptor 2 (EpHA2; cat. no. 6997), phosphorylated (p-)EpHA2^{Ser897} (cat. no. 6347), 3-phosphoinositide-dependent kinase 1 (PDK1; cat. no. 3062), p-PDK1^{Ser241} (cat. no. 3061), AKT (cat. no. 9272), p-AKT^{Ser473} (cat. no. 4060), mTOR (cat. no. 2972), mTOR^{Ser2448} (cat. no. 2971), P70s6k (cat. no. 9202), p-P70s6k^{Thr389} (cat. no. 9234), ERK (cat. no. 9102), p-ERK$^{Thr202/Tyr204}$ (cat. no. 9101) and vimentin (cat. no. 5741) antibodies were purchased from Cell Signaling Technologies, Inc. VEGF-A (cat. no. ab1316) antibodies were purchased from Abcam. Matrix metalloproteinase (MMP)-2 (cat. no. AB19167), MMP-9 (cat. no. AB19016) and Laminin 5γ2 (cat. no. MAB19562) antibodies were purchased from Millipore. Matrigel was purchased from BD Biosciences. Anti-mouse (cat. no. 115-035-062) and anti-rabbit (cat. no. 111-035-045) IgGs were purchased from Jackson ImmunoResearch Laboratories, Inc. Doxazosin (cat. no. D9815), thiazolyl blue tetrazolium blue (MTT; cat. no. M2128) and sulforhodamine B (SRB; cat. no. S9012) were purchased from Sigma-Aldrich.

Cell culture. A549 cells were cultured in RPMI 1640 medium supplemented with 10% (v/v) FBS and 1% (v/v) penicillin-streptomycin-amphotericin B solution. Cell cultures were maintained in a 37˚C incubator with 5% CO_2. Adherent cell cultures were passaged using 0.05% trypsin-EDTA after reaching ~80% confluence.

MTT assay. After a 24-h treatment with the indicated concentrations of doxazosin, the cells were incubated with MTT (final concentration 0.5 mg/ml) for 2 h. Then, the medium was removed and replaced with 100 µl DMSO to dissolve the formed purple formazan. An ELISA reader (570 nm) was used to assess the absorbance values (25).

SRB assay. Firstly, cells were seeded into 96-well plates. After overnight incubation, cells in partial wells were fixed with 10% trichloroacetic acid (TCA) for 10 min at room temperature and washed with ddH_2O. Cells at this stage represented the cell population at the time of drug addition (T0). The other cells were treated with (Tx) or without [control (C) in 0.1% DMSO] the indicated concentrations of doxazosin for an additional 48 h. Then, the cells (T0 and Tx) were fixed with 10% TCA for 10 min at room temperature and washed with ddH_2O. All cells were stained with 0.4% (w/v) SRB in 1% acetic acid for 10 min at room temperature, and then washed with 1% acetic acid to remove unbound dye. SRB bound cells were solubilized with 10 mM trizma base. Using the absorbance (515 nm) measurements for T0, C and Tx, the percentage of doxazosin effect was calculated as follows: [1-(Tx-T0)/(C-T0)] x100% (26,27).

Flow cytometry with propidium iodide (PI) staining. Cells were harvested by trypsinization, fixed with 70% (v/v) ethanol for 30 min at 4˚C and washed with PBS. The cells were then centrifuged at 500 x g for 10 min at room temperature and re-suspended with 0.3 ml PI solution containing Triton X-100 (0.1%, v/v), RNase (100 µg/ml) and PI (80 µg/ml). The cellular DNA content was analyzed using an FACScan flow cytometer and CellQuest software (V6.0.4; Becton, Dickinson and Company) (28).

VM formation assays. VM formation assays were performed in 48-well culture plates coated with 100 µl Matrigel (9.5 mg/ml). Following Matrigel polymerization at 37˚C for 30 min, the cells were seeded at $3.2x10^5$ cells/ml in serum-free RPMI medium onto the Matrigel. After cell adhesion to the Matrigel for 4 h (basal condition, representing non-VM forming condition), 0 or 25 µM doxazosin was added to the serum-free medium and a medium change *was* performed every 2 days at 37˚C for the indicated time, before western blotting and microscopic examination.

Periodic acid Schiff (PAS) staining and confocal microscopy. Cells were cultured on 18x18 mm glass coverslips coated with Matrigel at 37˚C for 30 min. After 72 h treatment with different concentration of doxazosin, 3D culture cells were fixed with 4% paraformaldehyde in PBS for 15 min at room temperature, then quickly washed with PBS. Vascular channels were stained using a PAS kit (cat. no. SI-395B; Sigma) for 10 min at room temperature, washed with PBS for 10 min and treated with Schiff reagent (cat. no. SI-395B; Sigma-Aldrich)

for 20 min at room temperature. The stained cells were washed with PBS for 15 min and vasculogenic morphogenesis was visualized using fluorescence microscopy (Zeiss Axio Imager, M1). Vascular channels were quantified using MetaMorph software (V7.8.0; Molecular Devices, LLC) (29). For 3D reconstruction, the 3D culture cells were stained with PAS and observed using a ZEISS Cell Observer SD Confocal Microscope (Zeiss GmbH) and ZEN software (V2.3; Zeiss GmbH) (30). The results were determined as follows: Total tube length=total length of tube (excluding nodes); mean tube length=(total tube length)/(number of segments); total tube area=total tube area (excluding nodes); mean tube area=(total tube area)/(number of segments); segments=total number of tube segments connecting branch points and/or ends. IC_{50} is the half maximal inhibitory concentration.

Reverse transcription-quantitative polymerase chain reaction (RT-qPCR). RT-qPCR were performed to assess mRNA expression levels. Corning Cell Recovery Solution (Corning, Inc.) was used to recover cells from 3D Matrigel cultures according to the manufacturer's instructions. Total RNA was extracted from the cells using an RNAspin Mini Kit (Cytivia), then cDNA was reverse transcribed from the total RNA (0.7 μg) using an iScript cDNA synthesis kit (Bio-Rad Laboratories, Inc.). The reverse transcription was performed at 37˚C for 60 min, and then at 85˚C for 5 min, according to the manufacturer's protocol. qPCR was performed using iTag Universal SYBR Green Supermix (Bio-Rad Laboratories, Inc.) and primer sequences as follows: Human *VEGF-A* forward (F), 5'-CTACCTCCACCATGCCAAGT-3' and reverse (R), 5'-GCAGTAGCTGCGCTGATAGA-3'; human *EPHA2* F, 5'-CCTCTAGTGCCTTCTTTAG-3' and R, 5'-GAATGTTTGACACCCTCT-3'; human *VE-cadherin* F, 5'-CGTGTTCGCCATTGAGAG-3' and R, 5'-TTCGCCAGTGTCCTTGTC-3'; human *N-cadherin* F, 5'-AGTACAGAAGCACTGGGATT-3' and R, 5'-AAGCGTGTTGAAGCATATCAT-3'; human *vimentin* F, 5'-AGTCCACTGAGTACCGGAGAC-3' and R, 5'-CATTTCACGCATCTGGCGTTC-3'; human *FAK* F, 5'-GTAGCGTGGCGTAAGTTA-3' and R, 5'-TTCCTTGACAAGTGAATTATGC-3'; and human *GAPDH* F, 5'-CAGGGCTGCTTTTAACTCTGGT-3' and R, 5'-GATTTTGGAGGGATCTCGCT-3'. DNA was amplified with an initial denaturation at 95˚C for 5 min, followed by 40 cycles of 95˚C for 5 sec, and 60˚C for 30 sec. GAPDH was chosen as the internal reference. The data were expressed as relative mRNA levels by Cq values and then subsequently converted to fold change (31).

Western blotting. Corning Cell Recovery Solution (Corning, Inc.) was used to recover cells from 3D Matrigel cultures according to the manufacturer's instructions. The cells were harvested, centrifuged at 500 x g for 10 min at 4˚C and lysed in 80 μl ice-cold lysis buffer (150 mM NaCl, 1% Triton X-100, 20 mM Tris-HCl pH 7.4, 1 mM EDTA, 1 mM EGTA, 1 mM PMSF, 10 μg/ml leupeptin, 1 mM Na_3VO_4, 1 mM NaF and 1 mM dithiothreitol) for 30 min. The concentration of the total protein was quantified using the Bradford method. Total protein was mixed with sample buffer and heated at 95˚C for 10 min. An equal amount of protein (30 μg) per lane was separated by 8 or 12% SDS-PAGE, transferred to PVDF membranes. The membrane was then blocked with 5% skimmed milk for 1 h at room temperature. Protein expression levels were detected with specific antibodies (1:1,000 dilution for the primary antibodies at 4˚C overnight and 1:7,000 dilution for the secondary antibodies at room temperature for 2 h). The membranes were washed three times with PBS-T (0.1% Tween 20) for 10 min after incubations with the primary and secondary antibodies. The immunoreactive proteins were detected with an enhanced chemiluminescence detection kit (LumiFlash™ Prime Chemiluminescent Substrate; cat. no. LF01-500; Visual Protein; Energenesis Biomedical Co., Ltd.) and the images were captured using a ChemiDoc™ MP System (Bio-Rad Laboratories, Inc.). Lab™ Software (V6.0; Bio-Rad Laboratories, Inc.) was used to semi-quantify the data from western blotting.

VEGF-A secretion quantification. ELISA was applied to assess VEGF-A secretion (32). 3D culture cells were treated with 25 μM doxazocin for 96 h. Then, the concentration of VEGF-A in the supernatant was determined using a Human VEGF Quantikine ELISA kit (cat. no. DEV00; R&D Systems, Inc.) according to the manufacturer's instructions.

MMP-2 secretion and quantification. 3D culture cells were treated with 25 μM doxazocin for 96 h. Then, the concentration of MMP-2 in the supernatant was determined using a Human MMP-2 Quantikine ELISA kit (cat. no. MMP200; R&D Systems, Inc.) according to the manufacturer's instructions.

Statistical analysis. Data are presented as the mean ± SEM. Student's unpaired t-test was performed for the statistical analysis of data comparing two groups. One-way ANOVA followed by the Bonferroni's post hoc test was used to perform the statistical analysis of multiple groups. $P<0.05$ was considered to indicate a statistically significant difference.

Results

3D tubular structures form in A549 cells. A Matrigel-based VM formation assay was performed to examine whether the NSCLC cell line, A549, generated channels in 3D cultures. The results demonstrated that the cells formed vessel-like structures when cultured on Matrigel (Fig. 1A). PAS staining was performed to identify the glycoprotein-rich inner area of VM vessels, and lumen-containing tubular structures were subsequently observed in cultures using confocal microscopy and ZEN software (Fig. 1A and Video S1) (30). VM-related gene expression levels were also determined. The results revealed that *VEGF-A* and *VE-cadherin* expression levels were markedly upregulated in VM-forming cells (Fig. 1B). *N-cadherin* and *vimentin* (EMT markers) levels were also increased in 3D cultures. In addition, the levels of *MMP-9*, which is responsible for cell motility and ECM remodeling (33), were raised. *MMP-2*, which is involved in degrading basement membrane components for cancer metastasis along with MMP-9 (33), expression levels showed an increased trend, albeit this was not significant. *FAK* expression was also increased, although not significantly These data demonstrated that glycoprotein-rich lined tubular structures and VM-related molecules were present in the constructed *in vitro* VM model.

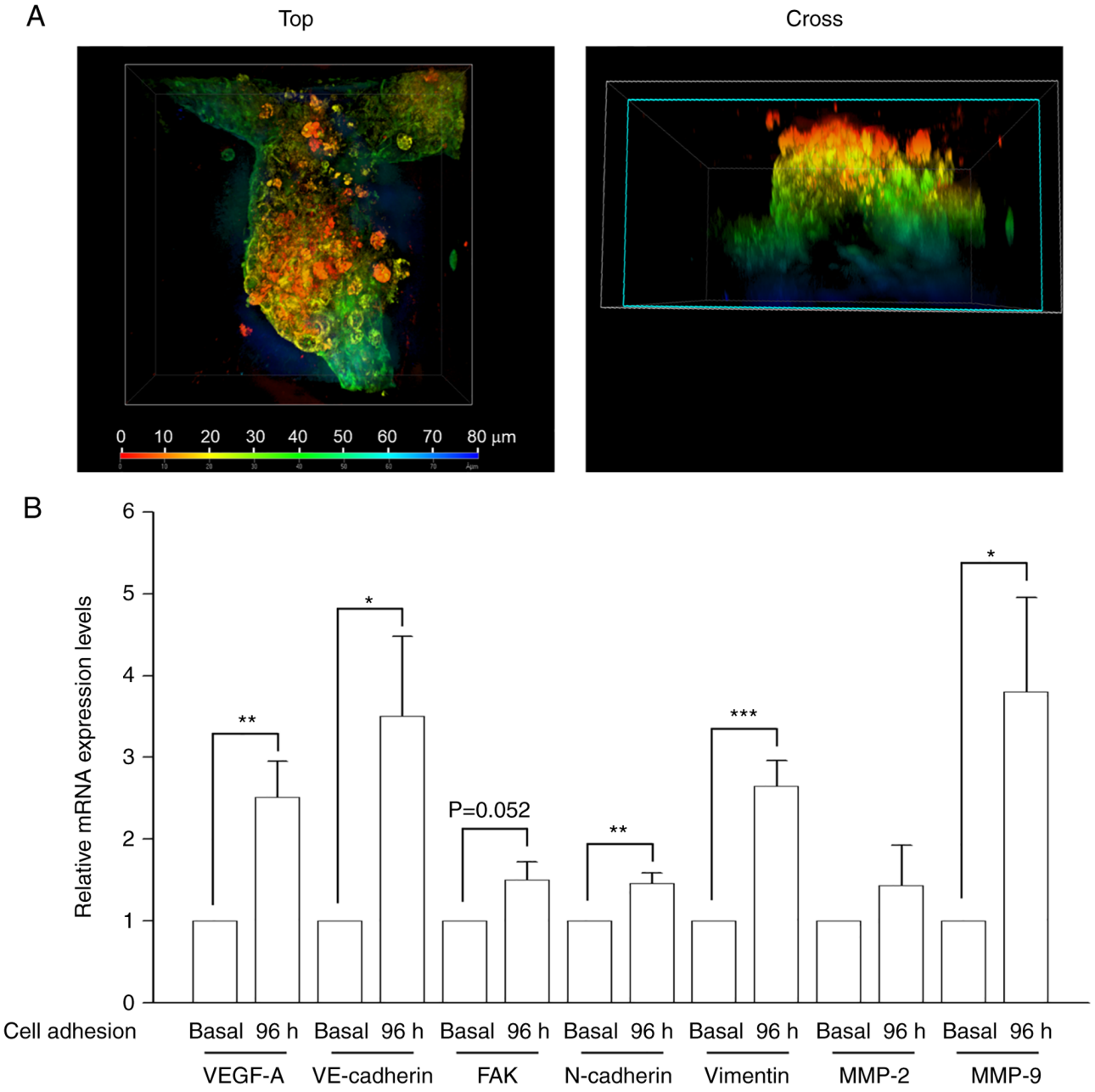

Figure 1. Characterization of a VM *in vitro* model of human non-small cell lung cancer. A549 cells were seeded in serum-free RPMI medium onto Matrigel and cultured for 96 h. Medium changes were performed every 2 days, then Corning Cell Recovery Solution was used to recover cells from the 3D Matrigel cultures. (A) Following Periodic Acid Schiff staining to identify the glycoprotein-rich inner area of VM vessels, 3D-reconstruction of a 6-day-old 3D culture of A549 cells was performed, with the resulting color map distinguishing between the planes and lumen-containing tubular structures present in the culture, using the confocal microscopy ZEN program. A view from the top and cross sections are shown. The cross section identified upper (red), middle (green) and lower sections (blue) of a tubular structure. (B) VM-related gene expression after a 96-h cell adhesion to Matrigel was determined by reverse transcription-quantitative polymerase chain reaction. Data are presented as the mean ± SEM of five experiments. *P<0.05, **P<0.01, ***P<0.001 compared with basal condition (cell adhesion to the Matrigel for 4 h). FAK, focal adhesion kinase; MMP, matrix metalloproteinase; VE-cadherin, vascular endothelial-cadherin; VEGF-A, vascular endothelial growth factor A; VM, vasculogenic mimicry.

Therefore, this model was utilized to evaluate the anti-VM effect of doxazosin.

Effect of doxazosin on VM formation. Quinazoline-based α_1-adrenergic receptor blockers are widely used therapeutic drugs for treating hypertension (34), one of which was examined in the present study using the constructed VM cell model. Vasculogenic morphogenesis on a Matrigel surface was visualized in the control group using fluorescence microscopy following PAS staining (Figs. 1A and 2A). Doxazosin inhibited capillary-like tube formation and caused a dispersed morphology in A549 cells (Fig. 2A). The total tube length, mean tube length, total tube area and mean tube area of mimetic vessels (quantified using MetaMorph software) were also reduced by doxazosin, with IC_{50} values of 36.07±1.38, 28.38±2.10, 31.27±0.32 and 24.17±2.35 μM, respectively (Fig. 2B). The results therefore indicated that doxazosin treatment of the 3D Matrigel cell culture model significantly reduced VM channel formation.

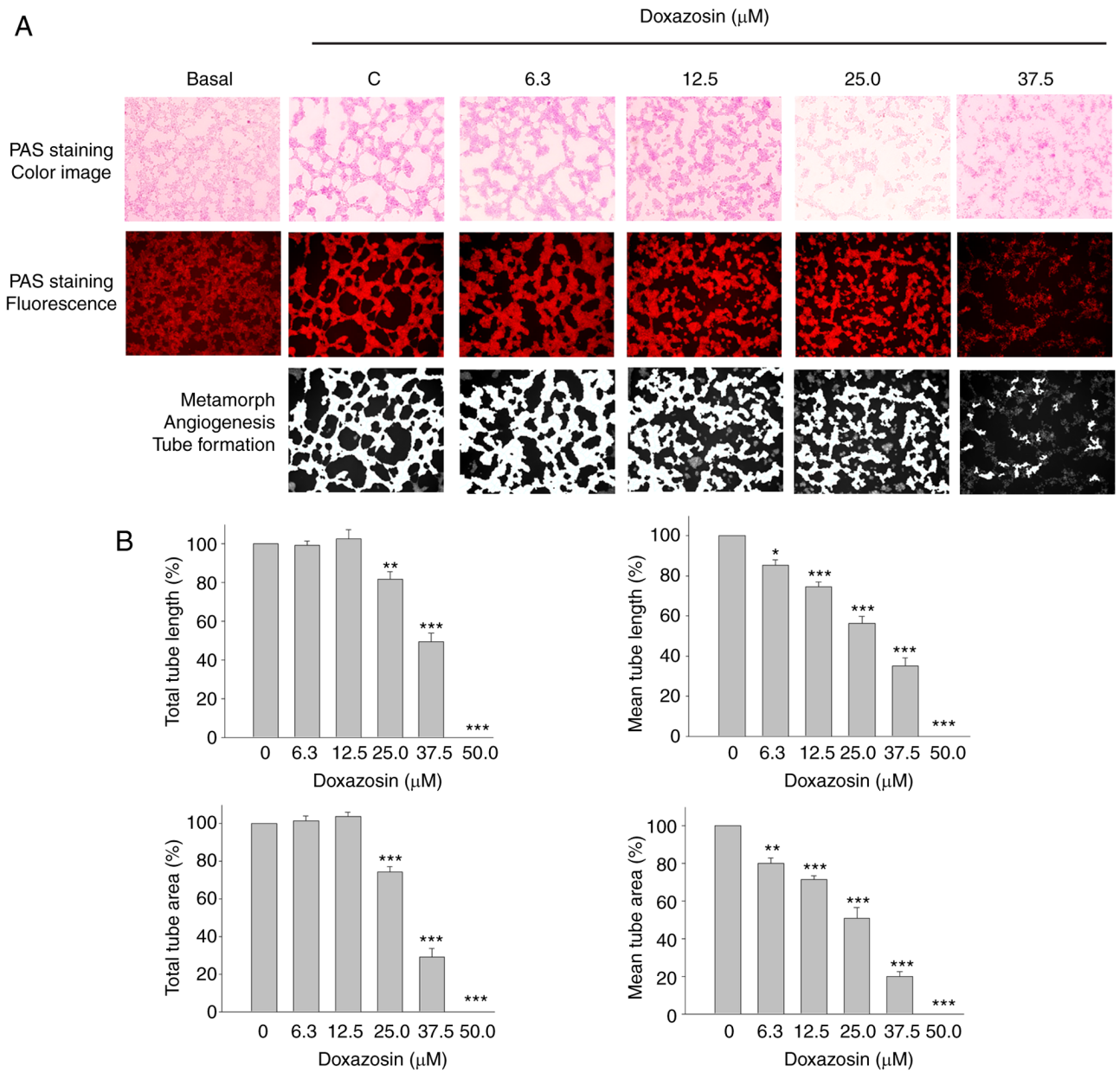

Figure 2. Effect of doxazosin on VM formation using PAS staining. A549 cells were seeded in serum-free RPMI medium onto Matrigel in the absence or presence of doxazosin for 72 h. Medium changes were performed every 2 days. (A) Following PAS staining to identify the glycoprotein-rich inner area of VM vessels, vasculogenic morphogenesis was visualized with using fluorescence microscopy (Zeiss AxioImager, M1) and (B) the results were quantified using MetaMorph software. Data are presented as the mean ± SEM of three experiments. *P<0.05, **P<0.01, ***P<0.001 compared with the control (0 μM doxazosin), determined using one-way ANOVA followed by the Bonferroni post hoc test. C, control; PAS, Periodic Acid Schiff; VM, vasculogenic mimicry.

Effect of doxazosin on cytotoxicity. The results of the SRB and MTT assays demonstrated that doxazosin also induced cytotoxic effects in A549 cells (Fig. 3). Doxazosin was more effective in inducing toxicities (6.3 μM, 13.1±4.6%; 12.5 μM, 20.8±5.6%; 25.0 μM, 45.1±3.5%; 37.5 μM, 98.2±9.1%) when using the SRB assay than when using MTT assay (cell survival: 37.5 μM, 72.6±4.4%; 50.0 μM, 47.8±1.8%; 100.0 μM, 14.5±0.1%) (Fig. 3A and B).

The effect of doxazosin on cell cycle progression was also examined, which revealed an increase in the apoptotic sub-G1 phase population with an initial apoptotic effect at 37.5 μM, compared with the 0 μM doxazosin control group (Figs. 3C and S1), which was similar to the aforementioned cytotoxicity assessment (Fig. 3B). The results therefore indicated that doxazosin was more effective in inducing anti-VM activities than in inducing cytotoxic effects.

Effect of doxazosin on VEGF-A and MMP-2 levels in 3D culture media. To further examine the doxazosin-mediated VM-blocking effect on underlying signaling pathways, the levels of two key mediators were determined in the medium during VM formation. The results revealed that the levels of both VEGF-A and MMP-2 in the control treatment group (0 μM doxazosin) were significantly increased compared with basal condition group, supporting VM formation (Fig. 4). Treatment with doxazosin significantly decreased these secretion levels.

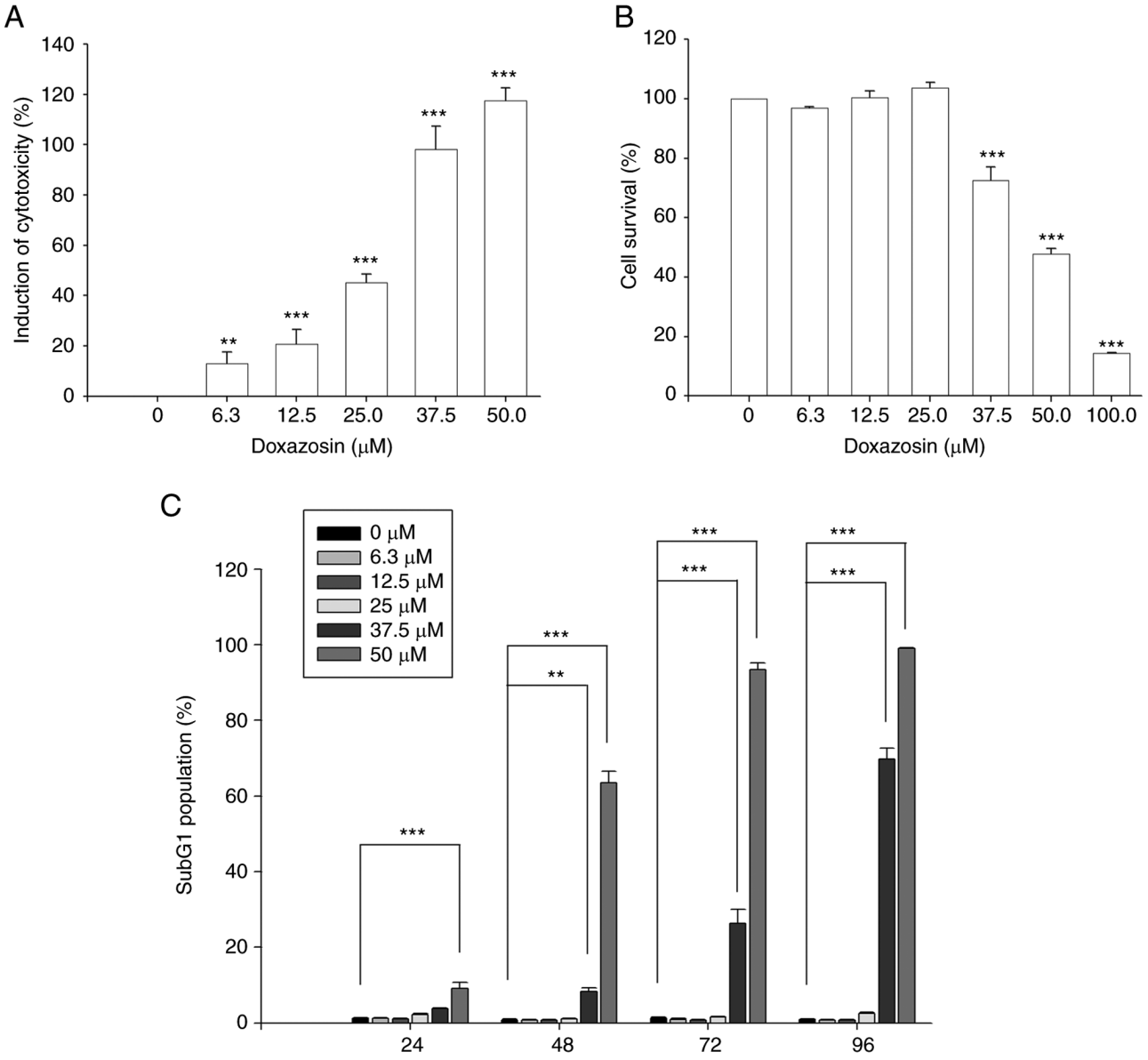

Figure 3. Effect of doxazosin on inducing cytotoxicity of A549 cells. A549 cells were incubated in the absence or presence of doxazosin. (A) After a 48-h treatment, the cells were fixed and then stained using Sulforhodamine B for the determination of the cytotoxicity. (B) After a 24-h treatment, the cells were stained using MTT for the determination of cell toxicity. (C) After the indicated treatment times, the cells were harvested for the detection of cell populations at different phases by propidium iodide staining and flow cytometry analysis. Data are presented as the mean ± SEM of three experiments. **P<0.01, ***P<0.001 compared with the control (0 μM doxazosin), determined using one-way ANOVA followed by the Bonferroni post hoc test.

Effect of doxazosin on the expression of pro-VM formation regulators. VE-cadherin is required for proper vascular development and is typically examined as an indicator of VM formation (35-39). VE-cadherin expression was significantly increased following a 96-h incubation of the 3D Matrigel cultures (Fig. S2). The VM-related protein expression levels were then examined following treatment with doxazosin. For this, A549 cells were seeded in serum-free RPMI medium onto Matrigel in the absence or presence of 25 μM doxazosin for 96 h. Then, Corning Cell Recovery Solution was used to recover cells from the 3D Matrigel cultures. The protein expression of several signaling pathways, including VEGF-A/VE-cadherin/p-EphA2/p-PDK1/p-AKT/p-mTOR/p-p70S6k/p-ERK, MMP-2/MMP-9/laminin 5γ2 and vimentin/fibronectin were determined by western blotting. Doxazosin markedly decreased the cellular protein expression of VEGF-A monomer and dimer (Fig. 5A). Furthermore, doxazosin significantly decreased the protein expression of VE-cadherin and EphA2, and significantly reduced the phosphorylation levels of PDK1, AKT, mTOR, P70S6K and ERK in the 3D Matrigel cell culture model (Fig. 5A). The aforementioned results revealed the doxazosin-mediated suppression of VM formation. MMP-2 and MMP-9 are reported to degrade collagen in the basement membrane, supporting remodeling of the ECM and the regulation of VM formation (40). Although the laminin 5γ2 chain is mainly cleaved by activated MMP-2 (not MMP-9) to produce the 5γ2' and 5γ2x cleaved fragments (which subsequently trigger the migration and invasion of tumor cells), both MMP-2 and MMP-9 colocalize with VM networks to assist VM formation (41). In the present study, doxazosin significantly reduced the protein expression levels of MMP-2 and MMP-9 and downregulated the protein expression levels

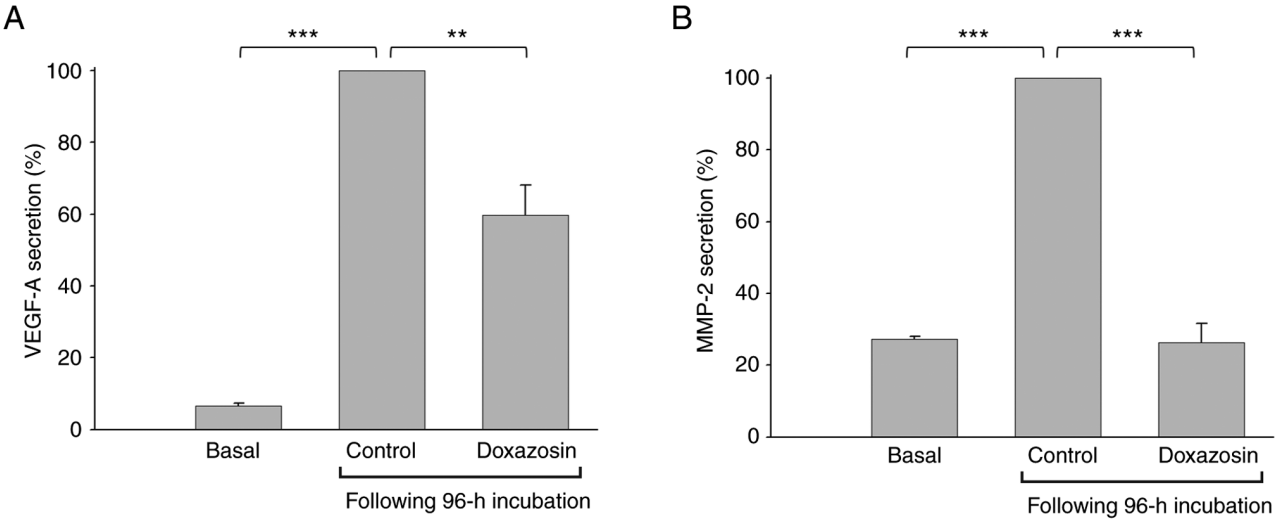

Figure 4. Effect of doxazosin on the secretion levels of VEGF-A and MMP-2 into the media during vasculogenic mimicry formation. A549 cells were seeded in serum-free RPMI medium onto Matrigel. After cell adhesion to the Matrigel for 4 h (basal condition), the cells were incubated in the absence or presence of 25 μM doxazosin for 96 h. The secretion levels of (A) VEGF-A (B) and MMP-2 were determined using commercial ELISA kits. Data are presented as the mean ± SEM of three experiments. One-way ANOVA by Bonferroni post hoc test is used to perform **P<0.01, ***P<0.001, compared with the control (0 μM doxazosin), determined using one-way ANOVA followed by the Bonferroni post hoc test. MMP-2, matrix metalloproteinase; VEGF-A, vascular endothelial growth factor A.

of the cleaved forms of laminin, 5γ2' and 5γ2x (Fig. 5B). EMT is reported to be implicated in VM formation and is associated with the tumor invasion-metastasis cascade (42). Doxazosin also significantly downregulated the protein expression levels of the two EMT markers, vimentin and fibronectin, in the 3D Matrigel-cultured A549 model (Fig. 5C). Collectively, these results confirmed that doxazosin displayed anti-VM activity in the NSCLC cell model.

Discussion

When tumors metastasize and grow in size, neovasculature is required to achieve sufficient nutrition through diffusion. VM serves as a mode of vascularization to mimic the vasculogenesis of endothelial cells (11,12,43). The vascular structure of VM has been reported to be built by cancer cells on rich ECMs, including proteoglycans and glycoproteins, which are positive for PAS staining. To identify VMs in human tumor biopsies and experimental settings, positive PAS staining in the absence of endothelial cell markers, such as CD31 or CD34, is generally used to assess vessel-like structures (30,43). However, certain studies raise an issue doubting the validity of concluding the presence of VM based solely on positive PAS staining without a definitive proof of a lumen in patterned vessel-like structures (44). In the present study, in accordance with the definition of VM formation, confocal microscopy examination was performed to detect structures with a lumen. The images showed lumen-like tubular structures after a 6-day growth of A549 cells in a Matrigel-cultured model. Furthermore, high PAS$^+$ staining of VM vessels was observed. Notably, the gene expression levels of *VEGF-A*, *VE-cadherin*, *N-cadherin*, *vimentin* and *MMP-9*, which are crucial molecules in driving VM formation (9,44), were also markedly increased. Collectively, these data indicated VM formation in the constructed 3D Matrigel-cultured A549 model.

Several anticancer mechanisms of doxazosin have been reported, including activation of DNA damage (45,46), the TGF-β pathway (47) and autophagy (20), and the inhibition of angiogenesis through regulating the VEGF/Akt/mTOR signaling (23). In the present study, the anti-VM effect of doxazosin was explored using the constructed NSCLC A549 model. Doxazosin displayed inhibitory activity, as demonstrated by the reduced PAS$^+$ staining of VM vessels and the quantified tube length and tube area. Notably, doxazosin was more efficient in blocking VM formation than inducing cytotoxicity by MTT assay and apoptosis. Although doxazosin induced similar anti-VM efficacy and cytotoxicity by SRB assay, the underlying mechanisms could be distinguished in which a broad panel of markers were used for anti-VM identification, including the protein expression of VEGF-A, MMP-2, MMP-9, VE-cadherin, EpHA2, vimentin and fibronectin, and laminin 5γ2 cleavage.

VE-cadherin is responsible for homotypic cell-cell interactions and vasculogenic events (48), and is exclusively expressed in highly aggressive tumors (49). Downregulation of VE-cadherin expression in aggressive melanoma cells abolished the ability to generate vasculogenic networks (49). Several studies have examined VE-cadherin as the only indicator for VM formation due to it having a prominent role in the acquisition of vascular-like structures (36-38). Recent research and review articles have also addressed the key role of VE-cadherin in VM formation (38,39). Hepatocellular carcinoma cells, cultured on plates coated with a fusion protein comprising a human VE-cadherin extracellular domain and an immunoglobulin G Fc region (hVE-cad-Fc), markedly formed patterned tubular structures and exhibited increased levels or activity of EphA2, MMP-2, MMP-9 and EMT makers (50). p-EphA2 has been reported to trigger PI3K and increase membrane type 1 matrix metalloproteinase/MMP/MMP-14 expression and MMP-2 activation through the FAK and ERK1/2 pathways (8). Subsequently,

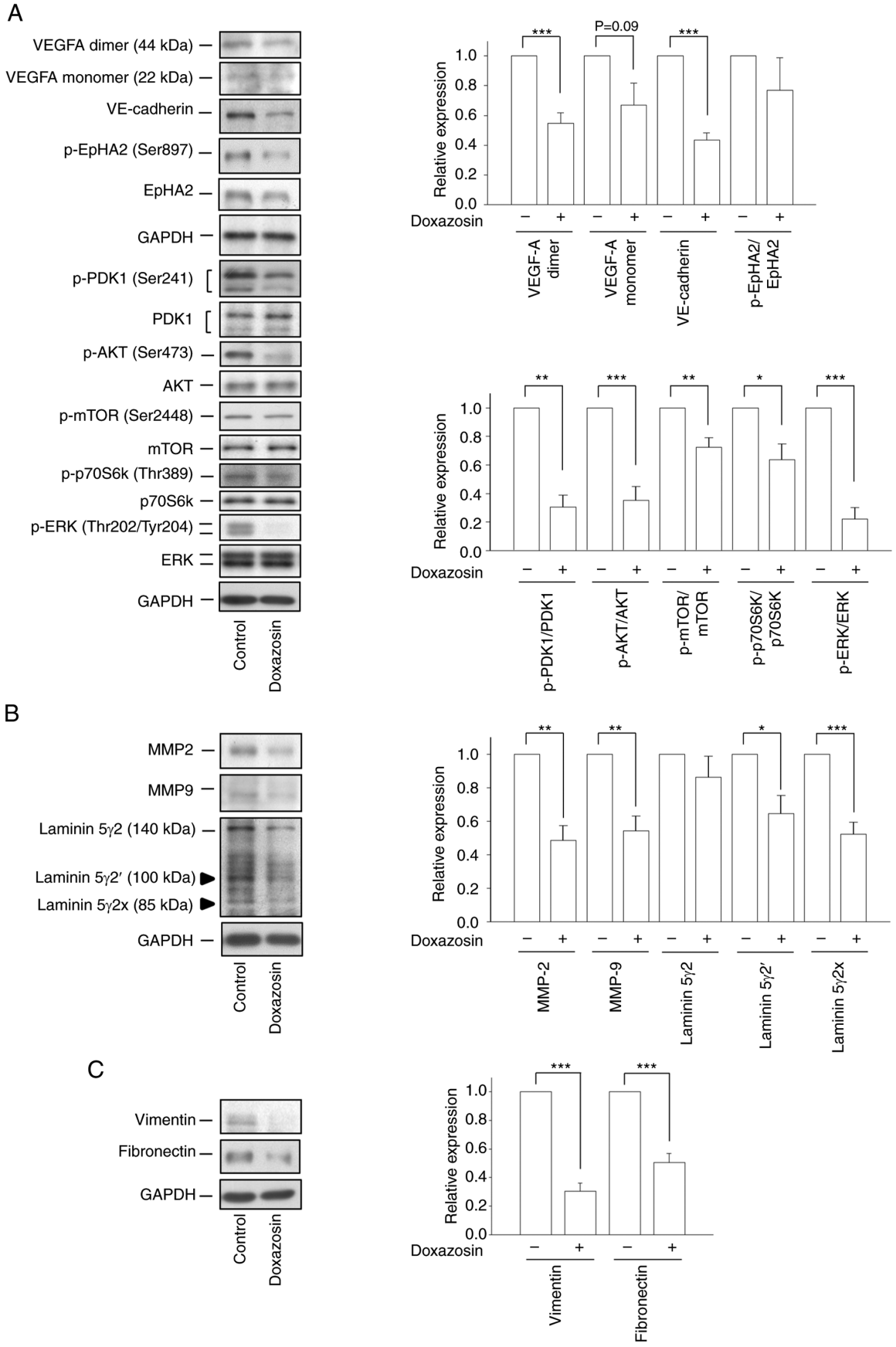

Figure 5. Effect of doxazosin on the expression of VM-related proteins. A549 cells were seeded in serum-free RPMI medium onto Matrigel in the absence or presence of 25 μM doxazosin for 96 h. Then, Corning Cell Recovery Solution was used to recover cells from the 3D Matrigel cultures. The protein expression levels of (A) VEGFA, VE-cadherin, p-EphA2, p-PDK1, p-AKT, p-mTOR, p-p70S6k, p-ERK, (B) MMP2, MMP9, laminin 5γ2, and (C) vimentin and fibronectin were determined by western blotting analysis. Data are presented as the mean ± SEM of three to five experiments. *P<0.05, **P<0.01, ***P<0.001, compared with the VM control (0 μM doxazosin). EphA2, Ephrin type-A receptor 2; MMP, matrix metalloproteinase; p-, phosphorylated; PDK1, 3-phosphoinositide-dependent kinase 1; VE-cadherin, vascular endothelial-cadherin; VEGF-A, vascular endothelial growth factor A; VM, vasculogenic mimicry.

the laminin 5γ2-chain is cleaved into γ2' and γ2x fragments that subsequently trigger migration, invasion and VM formation in melanoma (8,41). Apatinib and its combination with melatonin are reported to decrease the expression of VE-cadherin and EphA2, and inhibit the phosphorylation of PI3K and AKT, leading to the inhibition of VM formation, survival and invasion of breast cancer stem cells (51). In the present study, similar inhibitory effects of doxazosin were observed on VM formation in the A549 model through the downregulation of VE-cadherin and the EphA2/PI3K/PDK-1/AKT/mTOR pathway. The downregulation of both MMP-2 and MMP-9 also contributed to the anti-VM mechanism. Furthermore, doxazosin significantly inhibited the generation of γ2' and γ2x fragments, further supporting its anti-VM capability.

VEGF-A is another key mediator in VM formation. Secreted as a dimer, VEGF-A binds to VEGFR-1, which is highly expressed in malignant tumor cells with the capacity to induce VM formation (52). VEGF-A exposure triggers VM formation in several types of cancer cells, such as ovarian carcinoma (53) and melanoma (54), through increased expression of VE-cadherin, EphA2, MMP-2 and MMP-9, indicating that VEGF-A can stimulate tumor cell plasticity (53). *VEGF* gene silencing was reported to reduce VM formation and impair the expression levels of MMP-2 and MMP-9 via the PI3K/AKT-dependent pathway (55). Moreover, the blockade of EphA2 expression or activity inhibits VEGF expression and related angiogenesis in animal models, suggesting a complex regulation of these key regulators (56,57). In the present study, it was demonstrated that the gene expression and medium content of VEGF-A were upregulated in VM-forming cells, which was consistent with the aforementioned previous studies. Following doxazosin treatment, the reduction in VEGF-A expression might partly contribute to the inhibition of downstream VM signaling. EMT-related regulatory proteins are upregulated in VM-forming cells, suggesting a positive association between EMT and VM (42). MMPs, secreted by tumor cells lining VM networks, serve an important role in modifying cell-to-cell junctions and cell-ECM interactions, in which the ECM facilitates tumor invasion and metastasis (40). Due to the downregulation of MMP-2, MMP-9, vimentin and fibronectin protein expression observed in the present study following doxazosin treatment, doxazosin was hypothesized to inhibit EMT pathways, although this requires further validation.

It is noteworthy that several small molecules including natural products, synthetic compounds and known therapeutic drugs display anticancer potential through the suppression of VM formation (58). Furthermore, certain VM formation signaling pathways are suppressed by these agents (59,60). For example, triptonide potently inhibits VM by reducing the expression of VE-cadherin (59). Combretastatin A-4 and the synthetic compound, DHPAC, inhibit AKT phosphorylation and decrease the expression levels of VEGF, MMP2, MMP9 and Laminin 5 in NSCLC cell models (60). Following validation of the EphA2 receptor as a new target for treating tumors dependent on angiogenesis and VM (61), a novel synthetic compound, UniPR505, has been developed as an antagonist of the EphA2 receptor (62). Similarly, the present study demonstrated that doxazosin reduced the levels of VEGF-A, MMP-2, MMP-9 and VE-cadherin and inhibited the EphA2/AKT/mTOR/Laminin-5γ2 signaling network. Collectively, these studies together with the results of the present study support that the doxazosin-mediated suppression of VM formation may be an addition to the anti-NSCLC activities. However, the limitation of the present study is that it is a mechanistic study using 3D cancer cell culture without the consideration of interactions between other cell types and environments, as with in real tissues.

In conclusion, the results of the present study suggested that doxazosin displayed anti-VM activity in a 3D A549 model through the downregulation of VEGF-A and VE-cadherin levels, and the suppression of signaling pathways in which the receptor tyrosine kinase, EphA2, protein kinases, AKT and mTOR, and proteases, MMP-2 and MMP-9, are involved. These data support the add-on anti-VM effect of doxazosin as a potential agent against NSCLC.

Acknowledgements

The authors would like to thank Ms. Hwa-Man Hsu (Imaging Core, First Core Labs, National Taiwan University College of Medicine, Taipei, Taiwan), for technical assistance in image acquisition and analysis.

Funding

This work was supported by grants from the National Science and Technology Council (grant no. NSTC 112-2320-B-255-014) and the Chang Gung University of Science and Technology (grant no. ZURPF3N0091).

Availability of data and materials

The data generated in the present study may be requested from the corresponding author.

Authors' contributions

JLH, LCH, CHH and JHG contributed to the conception and design of the experiments. JLH performed the experiments. JLH and WJL analyzed the data. JLH, WJL and JHG confirm the authenticity of all the raw data. JLH and JHG wrote the manuscript. All authors read and approved the final version of the manuscript.

Ethics approval and consent to participate

Not applicable.

Patient consent for publication

Not applicable.

Competing interests

The authors declare that they have no competing interests.

References

1. Siegel RL, Miller KD, Wagle NS and Jemal A: Cancer statistics, 2023. CA Cancer J Clin 73: 17-48, 2023.
2. Li S, de Camargo Correia GS, Wang J, Manochakian R, Zhao Y and Lou Y: Emerging targeted therapies in advanced non-small-cell lung cancer. Cancers (Basel) 15: 2899, 2023.
3. Tan AC and Tan DSW: Targeted therapies for lung cancer patients with oncogenic driver molecular alterations. J Clin Oncol 40: 611-625, 2022.
4. Alexander M, Kim SY and Cheng H: Update 2020: Management of non-small cell lung cancer. Lung 198: 897-907, 2020.
5. Jurišić V, Obradovic J, Pavlović S and Djordjevic N: Epidermal growth factor receptor gene in non-small-cell lung cancer: The importance of promoter polymorphism investigation. Anal Cell Pathol (Amst) 2018: 6192187, 2018.
6. Jurisic V, Obradovic J, Nikolic N, Javorac J, Perin B and Milasin J: Analyses of $P16^{INK4a}$ gene promoter methylation relative to molecular, demographic and clinical parameters characteristics in non-small cell lung cancer patients: A pilot study. Mol Biol Rep 50: 971-979, 2023.
7. Sun R, Hou Z, Zhang Y and Jiang B: Drug resistance mechanisms and progress in the treatment of EGFR-mutated lung adenocarcinoma. Oncol Lett 24: 408, 2022.
8. Kirschmann DA, Seftor EA, Hardy KM, Seftor RE and Hendrix MJ: Molecular pathways: Vasculogenic mimicry in tumor cells: Diagnostic and therapeutic implications. Clin Cancer Res 18: 2726-2732, 2012.
9. Cao Z, Bao M, Miele L, Sarkar FH, Wang Z and Zhou Q: Tumour vasculogenic mimicry is associated with poor prognosis of human cancer patients: A systemic review and meta-analysis. Eur J Cancer 49: 3914-3923, 2013.
10. Hendrix MJ, Seftor EA, Hess AR and Seftor RE: Vasculogenic mimicry and tumour-cell plasticity: Lessons from melanoma. Nat Rev Cancer 3: 411-421, 2003.
11. van der Schaft DW, Seftor RE, Seftor EA, Hess AR, Gruman LM, Kirschmann DA, Yokoyama Y, Griffioen AW and Hendrix MJ: Effects of angiogenesis inhibitors on vascular network formation by human endothelial and melanoma cells. J Natl Cancer Inst 96:1473-1477, 2004.
12. Angara K, Rashid MH, Shankar A, Ara R, Iskander A, Borin TF, Jain M, Achyut BR and Arbab AS: Vascular mimicry in glioblastoma following anti-angiogenic and anti-20-HETE therapies. Histol Histopathol 32: 917-928, 2017.
13. Song H, Ci H, Xu J, Xu Z, Zhang Y, Wang Y, Wu S and Tao Y: Vasculogenic mimicry and expression of slug and vimentin correlate with metastasis and prognosis in non-small cell lung cancer. Int J Clin Exp Pathol 11: 2749-2758, 2018.
14. Ci H, Xu Z, Xu J, Wang Y and Wu S: Expressions of KAI1 and E-cadherin in nonsmall cell lung cancer and their correlation with vasculogenic mimicry. Medicine (Baltimore) 97: e12293, 2018.
15. Zhou X, Gu R, Han X, Wu G and Liu J: Cyclin-dependent kinase 5 controls vasculogenic mimicry formation in non-small cell lung cancer via the FAK-AKT signaling pathway. Biochem Biophys Res Commun 492: 447-452, 2017.
16. Naeem A, Dakshanamurthy S, Walthieu H, Parasido E, Avantaggiati M, Tricoli L, Kumar D, Lee RJ, Feldman A, Noon MS, *et al*: Predicting new drug indications for prostate cancer: The integration of an in silico proteochemometric network pharmacology platform with patient-derived primary prostate cells. Prostate 80: 1233-1243, 2020.
17. Dalwadi SM, Hunt A, Bonnen MD and Ghebre YT: Computational approaches for drug repurposing in oncology: Untapped opportunity for high value innovation. Front Oncol 13: 1198284, 2023.
18. Wu H, Huang D, Zhou H, Sima X, Wu Z, Sun Y, Wang L, Ruan Y, Wu Q, Wu F, *et al*: Metformin: A promising drug for human cancers. Oncol Lett 24: 204, 2022.
19. Pantziarka P, Pirmohamed M and Mirza N: New uses for old drugs. BMJ 361: k2701, 2018.
20. Batty M, Pugh R, Rathinam I, Simmonds J, Walker E, Forbes A, Anoopkumar-Dukie S, McDermott CM, Spencer B, Christie D and Chess-Williams R: The role of α1-Adrenoceptor antagonists in the treatment of prostate and other cancers. Int J Mol Sci 17: 1339, 2016.
21. Forbes A, Anoopkumar-Dukie S, Chess-Williams R and McDermott C: Relative cytotoxic potencies and cell death mechanisms of α1-adrenoceptor antagonists in prostate cancer cell lines. Prostate 76: 757-766, 2016.
22. Bilbro J, Mart M and Kyprianou N: Therapeutic value of quinazoline-based compounds in prostate cancer. Anticancer Res 33: 4695-4700, 2013.
23. Keledjian K, Garrison JB and Kyprianou N: Doxazosin inhibits human vascular endothelial cell adhesion, migration, and invasion. J Cell Biochem 94: 374-388, 2005.
24. Park MS, Kim BR, Dong SM, Lee SH, Kim DY and Rho SB: The antihypertension drug doxazosin inhibits tumor growth and angiogenesis by decreasing VEGFR-2/Akt/mTOR signaling and VEGF and HIF-1α expression. Oncotarget 5: 4935-4944, 2014.
25. Scherbakov AM, Vorontsova SK, Khamidullina AI, Mrdjanovic J, Andreeva OE, Bogdanov FB, Salnikova DI, Jurisic V, Zavarzin IV and Shirinian VZ: Novel pentacyclic derivatives and benzylidenes of the progesterone series cause anti-estrogenic and antiproliferative effects and induce apoptosis in breast cancer cells. Invest New Drugs 41: 142-152, 2023.
26. Jurisic V, Bogdanovic G, Kojic V, Jakimov D and Srdic T: Effect of TNF-alpha on Raji cells at different cellular levels estimated by various methods. Ann Hematol 85: 86-94, 2006.
27. Skehan P, Storeng R, Scudiero D, Monks A, McMahon J, Vistica D, Warren JT, Bokesch H, Kenney S and Boyd MR: New colorimetric cytotoxicity assay for anticancer-drug screening. J Natl Cancer Inst 82: 1107-1112, 1990.
28. Jurisic V, Srdic-Rajic T, Konjevic G, Bogdanovic G and Colic M: TNF-α induced apoptosis is accompanied with rapid CD30 and slower CD45 shedding from K-562 cells. J Membr Biol 239: 115-122, 2011.
29. Shaifer CA, Huang J and Lin PC: Glioblastoma cells incorporate into tumor vasculature and contribute to vascular radioresistance. Int J Cancer 127: 2063-2075, 2010.
30. Racordon D, Valdivia A, Mingo G, Erices R, Aravena R, Santoro F, Bravo ML, Ramirez C, Gonzalez P, Sandoval A, *et al*: Structural and functional identification of vasculogenic mimicry in vitro. Sci Rep 7: 6985, 2017.
31. Livak KJ and Schmittgen TD: Analysis of relative gene expression data using real-time quantitative PCR and the 2(-Delta Delta C(T)) Method. Methods 25: 402-408, 2001.
32. Jurisic V: Multiomic analysis of cytokines in immuno-oncology. Expert Rev Proteomics 17: 663-674, 2020.
33. Cabral-Pacheco GA, Garza-Veloz I, Castruita-De la Rosa C, Ramirez-Acuña JM, Perez-Romero BA, Guerrero-Rodriguez JF, Martinez-Avila N and Martinez-Fierro ML: The roles of matrix metalloproteinases and their inhibitors in human diseases. Int J Mol Sci 21: 9739, 2020.
34. Vincent J, Elliott HL, Meredith PA and Reid JL: Doxazosin, an alpha 1-adrenoceptor antagonist: Pharmacokinetics and concentration-effect relationships in man. Br J Clin Pharmacol 15: 719-725, 1983.
35. Franco P, Camerino I, Merlino F, D'Angelo M, Cimmino A, Carotenuto A, Colucci-D'Amato L and Stoppelli MP: αV-Integrin-Dependent inhibition of glioblastoma cell migration, invasion and vasculogenic mimicry by the uPAcyclin decapeptide. Cancers (Basel) 15: 4775, 2023.
36. Qin Y, Zhao W, Cai Z, Wang Q, Gao J, Ci H, Feng Z and Ma L: The biomarker like the correlation between vasculogenic mimicry, vascular endothelial cadherin, sex-determiningregion on Y-Box transcription factor 17, and cyclin D1 in oesophageal squamous cell carcinoma. J Oncol 2022: 8915503, 2022.
37. Zhang Y, Tan Y, Liu S, Yin H, Duan J, Fan L, Zhao X and Jiang B: Implications of Withaferin A for the metastatic potential and drug resistance in hepatocellular carcinoma cells via Nrf2-mediated EMT and ferroptosis. Toxicol Mech Methods 33: 47-55, 2023.
38. Delgado-Bellido D, Garcia-Diaz A and Oliver FJ: Co-immunoprecipitation of protein complexes from different subcellular compartments in vasculogenic mimicry studies. Methods Mol Biol 2514: 61-72, 2022.
39. Delgado-Bellido D, Oliver FJ, Vargas Padilla MV, Lobo-Selma L, Chacón-Barrado A, Díaz-Martin J and de Álava E: VE-Cadherin in cancer-associated angiogenesis: A deceptive strategy of blood vessel formation. Int J Mol Sci 24: 9343, 2023.
40. Winkler J, Abisoye-Ogunniyan A, Metcalf KJ and Werb Z: Concepts of extracellular matrix remodelling in tumour progression and metastasis. Nat Commun 11: 5120, 2020.
41. Seftor RE, Seftor EA, Koshikawa N, Meltzer PS, Gardner LM, Bilban M, Stetler-Stevenson WG, Quaranta V and Hendrix MJ: Cooperative interactions of laminin 5 gamma2 chain, matrix metalloproteinase-2, and membrane type-1-matrix/metalloproteinase are required for mimicry of embryonic vasculogenesis by aggressive melanoma. Cancer Res 61: 6322-6327, 2001.

42. Liu Q, Qiao L, Liang N, Xie J, Zhang J, Deng G, Luo H and Zhang J: The relationship between vasculogenic mimicry and epithelial-mesenchymal transitions. J Cell Mol Med 20: 1761-1769, 2016.
43. Maniotis AJ, Folberg R, Hess A, Seftor EA, Gardner LM, Pe'er J, Trent JM, Meltzer PS and Hendrix MJ: Vascular channel formation by human melanoma cells in vivo and in vitro: Vasculogenic mimicry. Am J Pathol 155: 739-752, 1999.
44. Valdivia A, Mingo G, Aldana V, Pinto MP, Ramirez M, Retamal C, Gonzalez A, Nualart F, Corvalan AH and Owen GI: Fact or fiction, it is time for a verdict on vasculogenic mimicry? Front Oncol 9: 680, 2019.
45. Lin SC, Chueh SC, Hsiao CJ, Li TK, Chen TH, Liao CH, Lyu PC and Guh JH: Prazosin displays anticancer activity against human prostate cancers: Targeting DNA and cell cycle. Neoplasia 9: 830-839, 2007.
46. Arencibia JM, Del Rio M, Bonnin A, Lopes R, Lemoine NR and López-Barahona M: Doxazosin induces apoptosis in LNCaP prostate cancer cell line through DNA binding and DNA-dependent protein kinase down-regulation. Int J Oncol 27: 1617-1623, 2005.
47. Partin JV, Anglin IE and Kyprianou N: Quinazoline-based alpha 1-adrenoceptor antagonists induce prostate cancer cell apoptosis via TGF-beta signalling and I kappa B alpha induction. Br J Cancer 88: 1615-1621, 2003.
48. Treps L, Le Guelte A and Gavard J: Emerging roles of Semaphorins in the regulation of epithelial and endothelial junctions. Tissue Barriers 1: e23272, 2013.
49. Hendrix MJ, Seftor EA, Meltzer PS, Gardner LM, Hess AR, Kirschmann DA, Schatteman GC and Seftor RE: Expression and functional significance of VE-cadherin in aggressive human melanoma cells: Role in vasculogenic mimicry. Proc Natl Acad Sci USA 98: 8018-8023, 2001.
50. Shuai Q, Cao L, Qin Z, Zhang Y, Gu Z and Yang J: VE-cadherin fusion protein substrate enhanced the vasculogenic mimicry capability of hepatocellular carcinoma cells. J Mater Chem B 8: 1699-1712, 2020.
51. Maroufi NF, Rashidi M, Vahedian V, Jahanbazi R, Mostafaei S, Akbarzadeh M, Kazemzadeh H, Nejabati HR, Isazadeh A, Rashidi MR and Nouri M: Effect of Apatinib plus melatonin on vasculogenic mimicry formation by cancer stem cells from breast cancer cell line. Breast Cancer 29: 260-273, 2022.
52. Frank NY, Schatton T, Kim S, Zhan Q, Wilson BJ, Ma J, Saab KR, Osherov V, Widlund HR, Gasser M, *et al*: VEGFR-1 expressed by malignant melanoma-initiating cells is required for tumor growth. Cancer Res 71: 1474-1485, 2011.
53. Wang JY, Sun T, Zhao XL, Zhang SW, Zhang DF, Gu Q, Wang XH, Zhao N, Qie S and Sun BC: Functional significance of VEGF-a in human ovarian carcinoma: Role in vasculogenic mimicry. Cancer Biol Ther 7: 758-766, 2008.
54. Vartanian A, Stepanova E, Grigorieva I, Solomko E, Baryshnikov A and Lichinitser M: VEGFR1 and PKCα signaling control melanoma vasculogenic mimicry in a VEGFR2 kinase-independent manner. Melanoma Res 21: 91-98, 2011.
55. Xu X, Zong Y, Gao Y, Sun X, Zhao H, Luo W and Jia S: VEGF induce vasculogenic mimicry of choroidal melanoma through the PI3k signal pathway. Biomed Res Int 2019: 3909102, 2019.
56. Cheng N, Brantley D, Fang WB, Liu H, Fanslow W, Cerretti DP, Bussell KN, Reith A, Jackson D and Chen J: Inhibition of VEGF-dependent multistage carcinogenesis by soluble EphA receptors. Neoplasia 5: 445-456, 2003.
57. Brantley-Sieders DM, Fang WB, Hwang Y, Hicks D and Chen J: Ephrin-A1 facilitates mammary tumor metastasis through an angiogenesis-dependent mechanism mediated by EphA receptor and vascular endothelial growth factor in mice. Cancer Res 66: 10315-10324, 2006.
58. Guan YY, Luan X, Lu Q, Liu YR, Sun P, Zhao M, Chen HZ and Fang C: Natural products with antiangiogenic and antivasculogenic mimicry activity. Mini Rev Med Chem 16: 1290-1302, 2016.
59. Han H, Du L, Cao Z, Zhang B and Zhou Q: Triptonide potently suppresses pancreatic cancer cell-mediated vasculogenic mimicry by inhibiting expression of VE-cadherin and chemokine ligand 2 genes. Eur J Pharmacol 818: 593-603, 2018.
60. Gong FL, Wang L, Yu LG, Dang YF, Jiang XN, Zhao L and Guo XL: DHPAC, a novel microtubule depolymerizing agent, suppresses angiogenesis and vasculogenic mimicry formation of human non-small cell lung cancer. J Cell Biochem 121: 4756-4771, 2020.
61. Margaryan NV, Strizzi L, Abbott DE, Seftor EA, Rao MS, Hendrix MJ and Hess AR: EphA2 as a promoter of melanoma tumorigenicity. Cancer Biol Ther 8: 279-288, 2009.
62. Incerti M, Russo S, Corrado M, Giorgio C, Ballabeni V, Chiodelli P, Rusnati M, Scalvini L, Callegari D, Castelli R, *et al*: Optimization of EphA2 antagonists based on a lithocholic acid core led to the identification of UniPR505, a new 3α-carbamoyloxy derivative with antiangiogenetic properties. Eur J Med Chem 189: 112083, 2020.